ELSEVIER

Journal of Wind Engineering
and Industrial Aerodynamics 90 (2002) 869–896

JOURNAL OF
wind engineering
AND
industrial
aerodynamics

www.elsevier.com/locate/jweia

On the determination of the aerodynamic coefficients of highway tunnels

Hong-Ming Jang[a,*], Falin Chen[b]

[a] *Department of Mechanical Engineering, Chinese Culture University, 111 Taipei, Taiwan, ROC*
[b] *Institute of Applied Mechanics, National Taiwan University, 107 Taipei, Taiwan, ROC*

Received 5 September 2001; received in revised form 5 February 2002; accepted 13 February 2002

Abstract

The determination of the aerodynamic coefficients of highway tunnels is crucial to set up an accurate theoretical model of tunnel ventilation. Their appropriate values vary with situations, such as traffic conditions, auxiliary facilities in tunnel, jet fan performance, and so on, and accordingly shall be determined in real situations. More importantly, their inherent situation-dependent characteristics shall be reflected in the model by using relevant aerodynamics and traffic data obtained by in situ measurement, instead of just employing the data obtained from reduced-scale experiments done in laboratory or the data obtained from handbooks. In this paper, we propose an optimization approach that can simultaneously determine the four major aerodynamic coefficients of road tunnels: the friction coefficient of tunnel wall, the averaged drag coefficients of small-sized and large-size vehicles, and the pressure-rise coefficient of jet fans. The approach is based on the data of the dynamic traffic as well as of the traffic-induced wind speed measured in the 1.8-km-long highway tunnel—Fu-De Tunnel located in the suburb of Taipei City. Since the measurement is made in a full-scale tunnel operating under various realistic traffic situations and Fu-De Tunnel is typical in the modern design, we believe that the coefficient values determined in this paper can be used directly in other modern highway tunnels and shall be more appropriate than those determined by other traditional ways.

1. Introduction

A tunnel ventilation system is designed to be able to supply enough fresh air for its users no matter the traffic is smooth or congested, and to provide proper smoke

*Corresponding author. Fax: +886-2-28615241.
E-mail address: hmjang@faculty.pccu.edu.tw (H.-M. Jang).

0167-6105/02/$ - see front matter
PII: S0167-6105(02)00156-3

controls in accidental fires, and also to suppress the possible temperature-rise in long tunnels caused by heavy traffic in hot summer afternoon [1]. In the design stage to examine if a tunnel ventilation system can achieve the expected functions mentioned above, one used to make analyses on the basis of an accurate mathematical model for the wind induced in the tunnel by the piston effect due to vehicular motion. Owing to the large aspect ratio of tunnels, the one-dimensional theoretical model has been proved to be one of the successful tools to compute the induced wind speed and other relevant physical quantities, such as temperature and smoke concentration [1–3]. The reliability of this model highly depends on the properness of the values of aerodynamic coefficients of the model, which include the friction coefficient (also known as Darcy friction factor) of tunnel wall, the drag coefficients of vehicles of different size, and the pressure-rise coefficient of jet fan. These coefficients are significant and may vary with the configuration of the auxiliary facilities in tunnel, traffic conditions in tunnel, and the surroundings of each jet fan so that it is better for them to be determined according to in situ measurement of some related data. However, the coefficient of entrance loss is less influential and does not vary significantly with different tunnel situations.

In most of the previous studies of tunnel ventilation (for example [1–3]), the values of these dynamical coefficients were obtained either from laboratory tests or by referring to handbooks. The traffic conditions employed in their studies were either simplified or conjectured so that their results may not reflect the real situation in road tunnels. For example, the drag coefficients of vehicles found in handbooks are usually measured for an individual vehicle under uniform flow, while in real situation the vehicle may move in the vortex shedding generated by other vehicles running ahead. Accordingly, the real value of drag coefficient varying with traffic condition is surely different from that measured in a laboratory. For another example, the friction coefficient of a road tunnel depends not only on the surface roughness of tunnel wall, but also highly on the configuration of auxiliary facilities (see Fig. 1). Therefore, its value shall be very different from those values determined experimentally for the pipes. Moreover, the pressure-rise coefficient of the jet fan found in the specification is also measured in the laboratory, whose environment is also very different from that of a real tunnel, so that its real value shall also be different from that shown in the specification.

Nowadays, due to the good progress of the measurement techniques on both the traffic flow (including the speed and the length of each vehicle, and the traffic density of each lane, and so on) as well as the induced wind speed, the determination of these aerodynamic coefficients in real situation has become possible. In this paper, we implement the in situ experiment in a highway tunnel and, based on the measured data, we propose a so-called optimization procedure to determine the most appropriate values of these aerodynamic coefficients in way of requiring the best agreement between the calculated and the measured transient wind speeds. To do this, we employ the so-called "traffic group-partition dilemma" [4] to convert the dynamic traffic flow into the pulsating induced wind speed through the numerical ventilation model. This calculated wind speed is then checked with the measured one, both are in the form of time series, to determine simultaneously the four

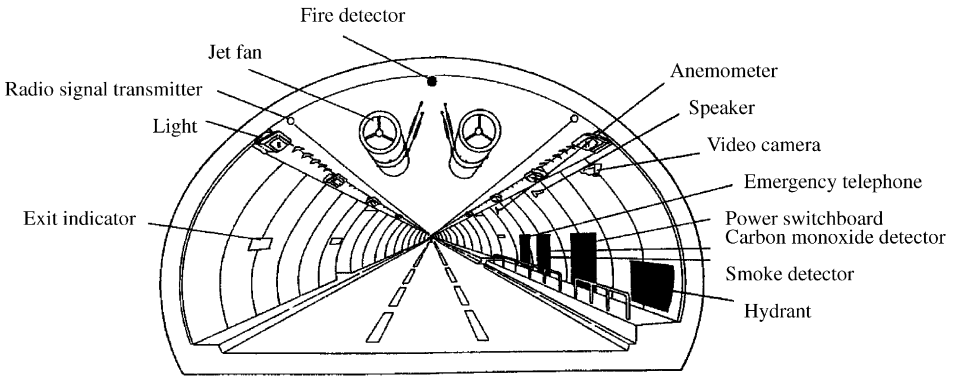

Fig. 1. Auxiliary facilities in Fu-De Tunnel (courtesy of Ministry of Transportation and Communications Taiwan Area National Expressway Engineering Bureau). On the wall of a road tunnel, there are not only the wall roughness elements but also the auxiliary facilities that poke through the thin viscous sublayer of the air flow; the drag, the pressure loss, and hence the friction coefficient depend on the configuration of these facilities.

aerodynamic coefficients. This optimization procedure can be applied to all the longitudinally ventilated highway tunnels because the numerical model is generally universal and the experiments are implemented in a typical tunnel of modern design.

In the following, the in situ measurement system is described in Section 2, in which discussions on the measured dynamic traffic flow and the pulsating wind speed are given. The mathematical model that bears the effects of the dynamic traffic flow is described in Section 3, in which an optimization procedure to determine the most appropriate values of the major aerodynamic coefficients and a hide-and-seek procedure to clearly explain the nature of the optimization procedure are also included. In Section 4, the optimization procedure is applied to determine the most appropriate values of the four aerodynamic coefficients from the measured traffic flow and the traffic-induced wind speed. Finally, concluding remarks are drawn in Section 5.

2. The in situ measurement

In this section, we will describe the in situ measurement system and discuss the measured traffic flow as well as traffic-induced wind speed.

2.1. The measurement system

The tunnel chosen for the in situ measurement is the Fu-De Tunnel [4], which locates in the suburb of Taipei City and is one of the long tunnels of the Northern Second Highway of Taiwan. The traffic of this highway is quite typical to the area of large population (there are more than four million habitants in this area): pretty heavy and serious traffic jam frequently happened in rush hours on a daily basis.

A measurement system was set up in this tunnel to measure the traffic flow at the outlet portal of the southbound tube and the induced wind speed at three locations: 50, 500, and 1000 m from the outlet portal. This system had been built in Fu-De Tunnel for about 4 years since March 1996 just before the highway was opened. In the beginning stage of our experiment, the major task was aimed at watching the traffic flow and the induced wind during a long period, such as a week or a month. Latter, the experiment was focused on capturing the transient features of both the traffic flow and the induced wind, especially for situations of congestion, accident, bad weather, etc. A remote data acquisition system was also added to the measurement system in the fourth year, so that the measured data could be downloaded from the computer on the university campus. Thus, the data acquisition task can be done in a more complete as well as larger scale. To know more details of the measurement system the reader is referred to references [1,4,5].

2.2. The measured traffic-flow data

The traffic flow measured on a typical weekday of 1997 is discussed in this section to reveal the variation of the traffic situation during a period of 16 h started from midnight. These data are then divided into some periods according to different averaged traffic densities so that each of them is suitable for performing the coefficient-optimization analysis.

First, the traffic at the outlet portal of the southbound tube of Fu-De Tunnel at 8:04 (8 O'clock and 4 min) on 4/13/2000 (April 13, 2000) is shown in Fig. 2. This photo was taken from the CCD camera used to measure the length, the speed of each vehicle, and to count the number of vehicles passing over each detection zone. One detection zone is defined for each lane in the image-process system. The vehicles are classified as small-sized, large-sized, and medium-sized vehicles as their measured lengths are, respectively, <7.6 m, >11 m, and in between. This photo reveals that most vehicles were sedans (small-sized vehicles) in this morning rush hour. The cargo truck showed up in the center of the photo, for example, is classified as a large-sized vehicle. This truck and the two sedans on the two sides happened to be in the detection zone of each lane. One can see from this photo that vehicles were lined up neatly in each lane, implying that in most situations vehicles move in the tunnel with the same manner.

The data were recorded for each lane in every time interval being set between 10 s and 60 min. Due to the fact that more than one vehicle may pass the detection zone during one time-interval, the measured traffic-flow data recorded therefore do not stand for each vehicle but for each group of vehicles (the number of vehicle of each group depends on the length of time interval). A vehicular group is defined as a group of vehicles of the same size passing the detection zone within the same time interval. With this definition, we can shorten the time interval so that the transient features of the traffic flow can be captured as clearly as possible. For the present measurement system, the shortest available time interval is 10 s. The data standing for the traffic flow are therefore the location, the averaged speed, and the number of vehicles of every vehicular group in every time interval. Based on these data, the total

Fig. 2. The view of the CCD camera, which shows the traffic at the outlet portal of the southbound tube of Fu-De Tunnel at 8:04, 2000/4/13. One detection zone is defined for each lane in the image-process system. The cargo truck and the two sedans on the two sides happened to be in the detection zone of each lane. The speed and the length of each vehicle and the number of vehicles passing through each detection zone are measured and recorded chronologically.

number of vehicular groups in the tunnel and the averaged speed as well as the averaged traffic density of each of these vehicular groups during each time interval can be calculated. These data can then be used in the numerical ventilation model to calculate the time series of the induced wind speed in the tunnel, and the associated pressure, temperature, and pollutant concentration along the tunnel as well [4,5].

Based on the approach described above, the traffic-flow data measured within 0:00–16:00 on 7/23/1997 are transformed into the number of vehicles in the tunnel and the averaged speed of these vehicles for each time interval of 10 s, as shown in Fig. 3(a). We see the averaged speed of the vehicles was around 90 km/h and was about 60 km/h in the morning rush hour. The traffic-flow data are used to calculate the averaged traffic density, as shown in Fig. 3(b). It is seen that in the worst situation the averaged traffic density was 23 vehicles/lane/km, or the averaged distance between two adjacent vehicles was about 43 m. This figure also shows that the percentage of small-sized vehicles in the daytime remained at around 90%, and

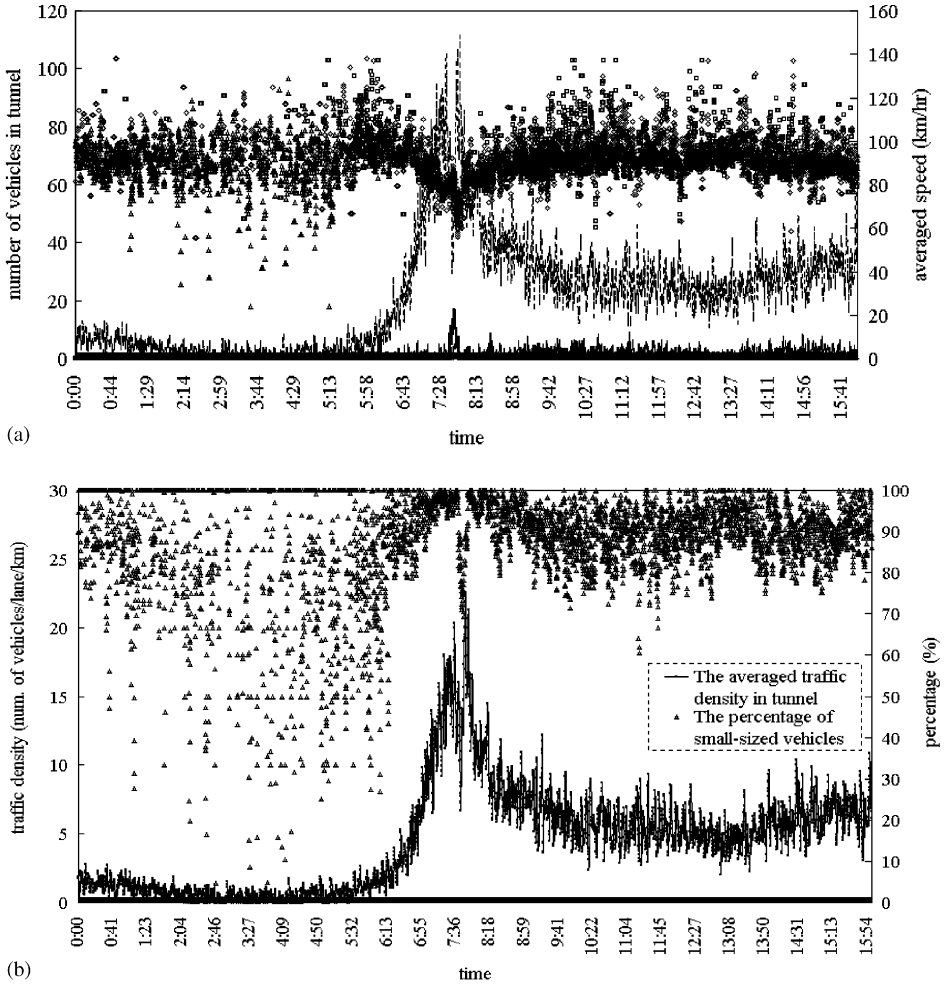

Fig. 3. The data that describe the traffic flow in Fu-De Tunnel on 7/23/1997. (a) The total number and averaged speed of vehicles in the tunnel. The zigzag lines, - - -, —, and ▬, respectively, indicate the total number of small-sized, medium-sized, and large-sized vehicles in the tunnel for every time interval of 10 s, while the marks, △, ◇, and, □ denote the averaged speed of the small-sized, medium-sized, and large-sized vehicles, respectively. (b) The traffic density and the percentage of small-sized vehicles in the tunnel.

was even higher during the rush hours, but was very low during the nighttime when large-sized trucks prevailed.

It is known that traffic flow plays a major role on inducing the wind in a tunnel by piston effect, which depends not only on the speed and the frontal area of each vehicle, but also on the traffic density as well. Fig. 3(b) shows that the traffic density in 0:00–6:00 was between 0 and 3 vehicles/lane/km, the traffic density in 10:00–16:00 was in the range 3–8 vehicles/lane/km, and that in 7:00–8:30 increased to 8–23

vehicles/lane/km. We accordingly divide these data into three groups of different traffic-density ranges. The optimization procedure is then to be performed for each group of data so that the corresponding aerodynamic coefficients can be determined.

2.3. The measured time series of wind speed in the tunnel

Since the discussion above has suggested us to divide the traffic-flow data into three groups, respectively, during 0:00–6:00, 7:00–8:30, and 10:00–16:00, we also divide the measured wind speed into three groups accordingly. The time series of wind speed measured in 0:00–6:00 and 10:00–16:00 are shown in Figs. 4(a) and (b), respectively, for revealing the accuracy of the measurement system. In both figures the wind speed measured by the two anemometers installed at, respectively, 500 and 50 m from the outlet portal are shown. Any one of the two time series measured at

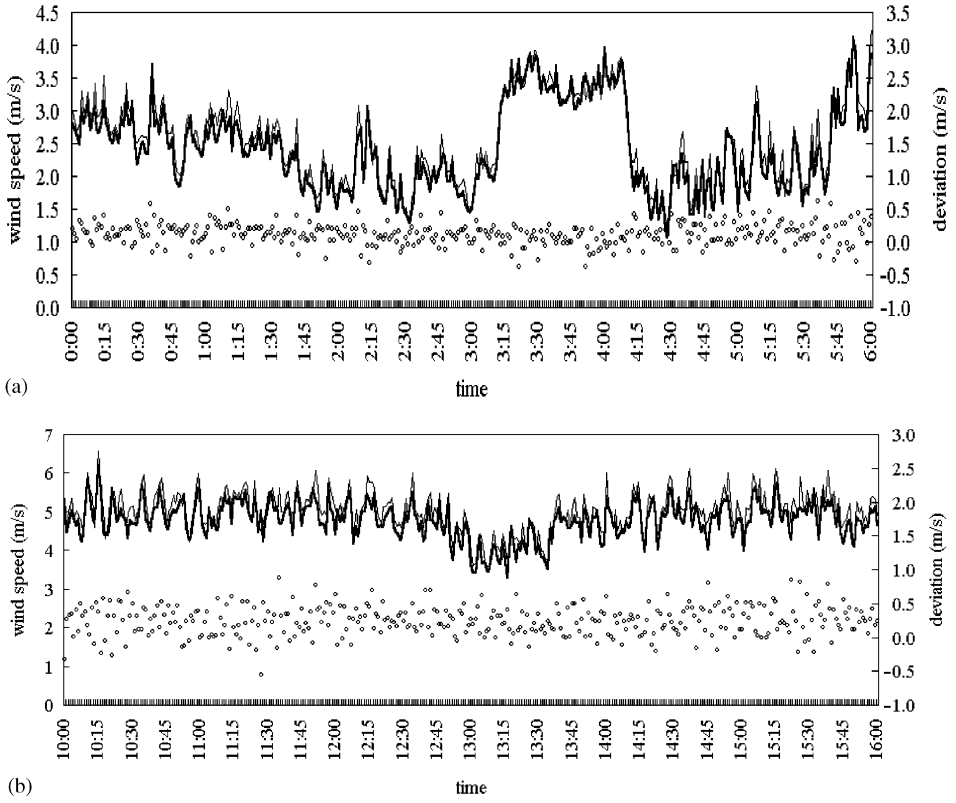

Fig. 4. Comparison of the time series of wind speed measured at two different locations in the tunnel on 7/23/1997. The zigzag lines —, and ▬▬, show the time series of wind speed measured at 500 and 50 m from the outlet portal, respectively. The small circles indicate the deviations between the two series. The consistency of the two time series is very good on magnitude, amplitude, and phase, which reveals the high accuracy of the wind-speed measurement system as well as the incompressibility nature of the flow.

different locations may be used as the standard time series for the optimization procedure. This is supported by the fact that the data measured at two different locations of 450 m apart are quite consistent in terms of magnitude, amplitude, and phase as well, implying that the standard series can be representative to the induced wind speed in the tunnel.

Either inherent factors or random happening factors, leading to errors of the experimental data, may influence the measured wind speed. These error-factors include the system error of instruments, the disturbance on flow around the anemometer caused by the large-sized vehicles passing by, the jet stream generated by the jet fan, and so on. The anemometers may not correctly measure the wind speed if these factors dominate. Fortunately, either Fig. 4(a) or (b) shows that the time series of wind speed, which were measured at two different locations, do not have any big difference, implying that the error-factors of both anemometers are insignificant. Since the error-factor is crucial to the optimization procedure, we propose in the following a statistical approach to quantitatively estimate the errors caused in measurements.

Since the wind-speed series of Figs. 4(a) and (b) were recorded once in every minute, there were 361 wind-speed values for each series in the 6-h period shown. Due to some inherent and random factors mentioned above, the two series of the wind speed measured at two different locations will have deviation, which at the ith minute is defined as

$$\varepsilon_i \equiv V_i - V_i^*, \quad i = 1, 2, \ldots, n. \tag{1}$$

In this equation, V_i^* and V_i denote the wind speed measured, respectively, by the two anemometers and n is the total number of data measured by each anemometer, which is 361 for the present case. The small circles of Figs. 4(a) and (b) indicate these deviation data, being confined to a limited range. Based on these data, their discrete probability densities can be calculated, as shown by the shaded circles of Figs. 5(a) and (b). A discrete probability density, $p_d(\varepsilon)$, is defined as $n_\varepsilon/n\Delta\varepsilon$, where n_ε is the number of deviation data whose values fall in the range $\varepsilon \pm \frac{1}{2}\Delta\varepsilon$ with $\Delta\varepsilon$ given by $(\varepsilon_{max} - \varepsilon_{min})/10$ and ε_{max} and ε_{min} denote the maximum and minimum deviation values, respectively. These deviation data are then sorted into 10 groups. The solid line of Fig. 5(a) represents the density of a normal distribution function with a mean deviation $\mu = 0.121$ m/s and a standard deviation $\sigma = 0.161$ m/s. The solid line of Fig. 5(b) represents the density of another normal distribution function with

Fig. 5. Discrete probability densities of the deviation between measured and calculated time series of wind speed in: (a) 0:00–6:00, (b) 10:00–16:00, and (c) 7:00–8:30, 7/23/1997. In these figures, shaded circles indicate the discrete probability densities of the deviation between the series of wind speed measured at 500 m from the outlet portal and the standard one, while outline circles indicate that between the calculated series of wind speed and the standard one. The time series of wind speed measured at 50 m from the outlet portal is served as the standard series. Either the dashed or the solid line represents the density of a normal distribution function. Each of the two lines coincides very well with each corresponding group of circles and reveals that the deviation between the two series compared is caused by random happening factors, such as vehicle shed vortices, uncertainties of vehicle frontal area and speed, etc.

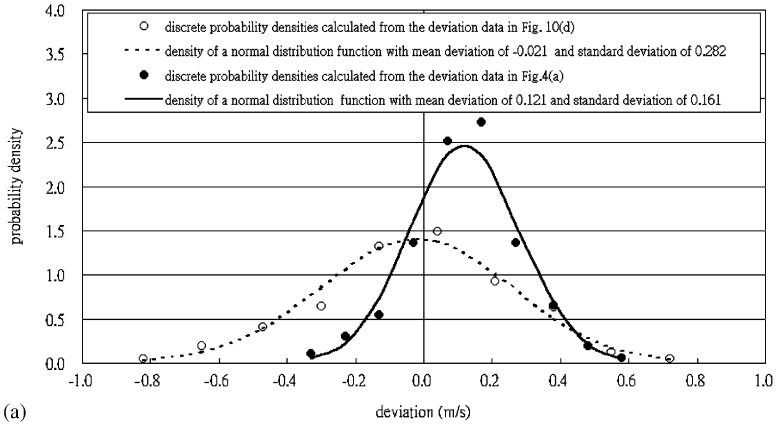
discrete probability densities calculated from the deviation data in Fig. 10(d)
density of a normal distribution function with mean deviation of -0.021 and standard deviation of 0.282
discrete probability densities calculated from the deviation data in Fig.4(a)
density of a normal distribution function with mean deviation of 0.121 and standard deviation of 0.161
probability density
deviation (m/s)

(a)

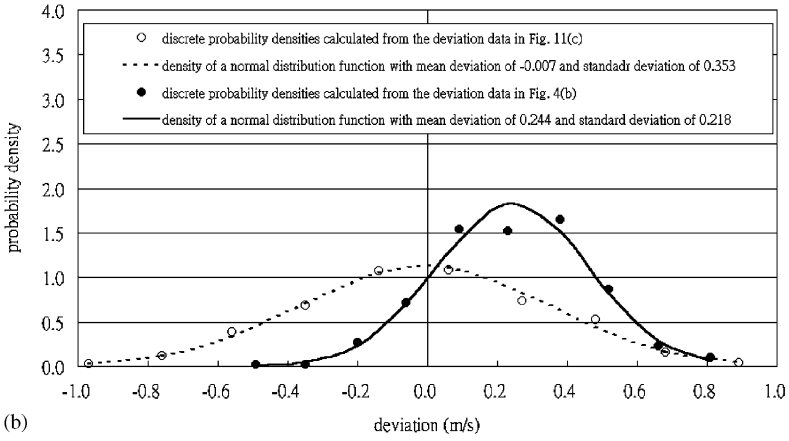
discrete probability densities calculated from the deviation data in Fig. 11(c)
density of a normal distribution function with mean deviation of -0.007 and standadr deviation of 0.353
discrete probability densities calculated from the deviation data in Fig. 4(b)
density of a normal distribution function with mean deviation of 0.244 and standard deviation of 0.218
probability density
deviation (m/s)

(b)

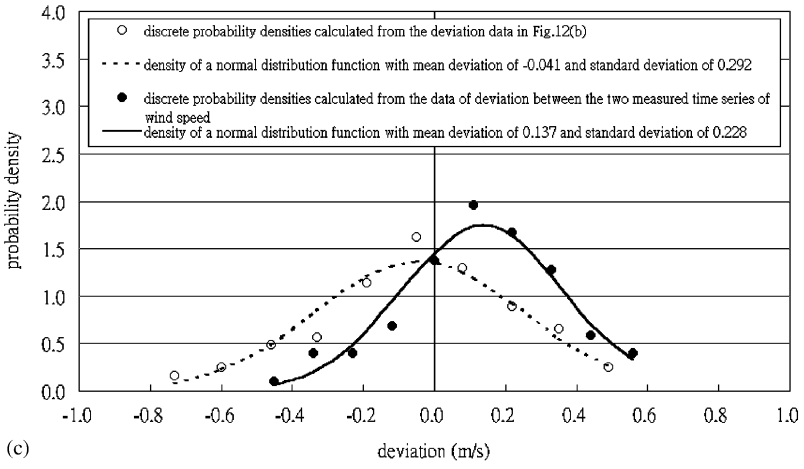
discrete probability densities calculated from the deviation data in Fig.12(b)
density of a normal distribution function with mean deviation of -0.041 and standard deviation of 0.292
discrete probability densities calculated from the data of deviation between the two measured time series of wind speed
density of a normal distribution function with mean deviation of 0.137 and standard deviation of 0.228
probability density
deviation (m/s)

(c)

$\mu = 0.244\,\mathrm{m/s}$ and $\sigma = 0.218\,\mathrm{m/s}$. The mean deviation and the standard deviation between the two measured time series of wind speed for a period of n minutes is defined by

$$\mu \equiv \sum_{i=1}^{n} \varepsilon_i / n \quad \text{and} \quad \sigma = \sqrt{\frac{1}{n-1}} \sum_{i=1}^{n} (\varepsilon_i - \mu)^2,$$

respectively [6]. By comparing those shaded circles and the solid line in either Fig. 5(a) or (b), we see the discrete probability densities of these wind-speed deviation data are rather close to that of a normal distribution function. Fig. 5(c), which is resulted from the measurement within 7:00–8:30, illustrates similar result although the total number of deviation data is as small as 91.

3. Mathematical model and optimization procedure

In this section, the one-dimensional mathematical model and the optimization procedure are described. The one-dimensional model is employed to compute the time series of wind speed based on the measured traffic-flow data. The optimization procedure is devised to determine the most appropriate aerodynamic coefficients that make the calculated series of wind speed to be best fitted to the measured standard series.

3.1. Mathematical model

The governing equation of the induced wind in the tunnel is as follows:

$$\sum_{i=1}^{5} F_i = \rho A_t L \frac{\mathrm{d}V}{\mathrm{d}t}, \tag{2}$$

where $F_i, i = 1-5$ are

$$F_1 = \sum_{j=1}^{J} \frac{\rho}{2} C d_j (U_j - V)|U_j - V| A v_j N v_j, \tag{3}$$

$$F_2 = -f \frac{\rho}{2} \frac{L}{D_h} A_t V|V|, \tag{4}$$

$$F_3 = (P_{in} - P_{out}) A_t, \tag{5}$$

$$F_4 = N_F \rho A_F |V_F| (V_F - V) K_j, \tag{6}$$

$$F_5 = -K_{en} \frac{\rho}{2} A_t V|V|. \tag{7}$$

In above equations, F_1 accounts for the vehicular piston force, F_2 the wall friction force, F_3 the force due to the pressure difference between the inlet and outlet portals, F_4 the fan thrust, and F_5 the additional friction force caused by the flow separation at the inlet portal. Among these forces, the vehicular piston force is the most

significant driving force making the tunnel wind speed pulsating. Moreover, ρ is the density of the air, A_t the cross-section area of tunnel, L the length of tunnel, t the time, V the induced wind speed, Cd_j the averaged drag coefficient of vehicles of group j, U_j the averaged speed of vehicles of group j, Av_j the averaged frontal area of vehicles of group j, and Nv_j the number of vehicles in group j, f the friction coefficient of tunnel, D_h the hydraulic diameter of tunnel, N_F number of jet fans in operation, A_F the discharging area of jet fan, V_F the discharging air speed of jet fan, K_j the pressure-rise coefficient of jet fan, and K_{en} the coefficient of entrance loss. P_{in} and P_{out} are the static pressures at the inlet portal and the outlet portal, respectively, which are related by

$$P_{in} = P_{out} - \frac{1}{2}\rho V^2 - \rho\sqrt{\frac{A_t}{2(\pi - \theta_h)}}\frac{dV}{dt}, \tag{8}$$

where θ_h is the elevation angle of the foothill slope around the inlet portal. The details of the derivation of Eq. (8) is shown in Appendix A.

To accurately calculate the induced wind speed in the tunnel, all the parameters in Eqs. (2)–(8) must be properly specified. Among them the values of ρ, A_t, L, D_h, N_F, A_F, V_F, and θ_h can be specified according to the design and operational specification of the tunnel. The values of U_j and Nv_j can be accurately calculated from the measured traffic-flow data. The value of Av_j can be determined according to the vehicle size detected by video image. The character J indicates total number of vehicular groups in the tunnel in each time interval and can be estimated from the measured vehicle speed through a procedure described in reference [4]. The values of parameters f, K_{en}, and K_j depend mostly on the design specification of the tunnel and the environment around those fans in action, and therefore can hardly be directly measured or specified but shall be determined on the basis of rigorous theoretical approach, as will be discussed below.

We note that although the exact value of K_{en} is unknown, its influence on the tunnel wind speed is very small [5,7]. Therefore, it is specified as 0.6 in our study, as usually used in the previous studies [3,8,9]. Except this, the other three coefficients f, K_j, and Cd_j are of large environment-dependency characteristics. For example, the value of friction coefficient f shall depend not only on the surface roughness of tunnel wall but also on the "roughness" formed by the auxiliary facilities of the tunnel (Fig. 1). As a result, the value of f shall be determined for the real full-scale tunnel. The values of Cd_j and K_j change with varying vehicles, traffic situations, and the flow around jet fans as well. Accordingly, these coefficients are determined by the optimization procedure described in the next section.

Although vehicles are sorted into three categories according to vehicle length by the measurement system, we find that the medium-sized and large-sized vehicles have approximately the same frontal area, which is obviously larger than that of the small-sized vehicles. For being able to count more accurately the piston force, the parameters Av_j and Cd_j are further separated into A_{vs} and Cd_s for small-sized vehicles and A_{vl} and Cd_l for the medium-sized and large-sized vehicles (these two kind of vehicles shall be categorized as large-sized vehicles thereafter). Previous

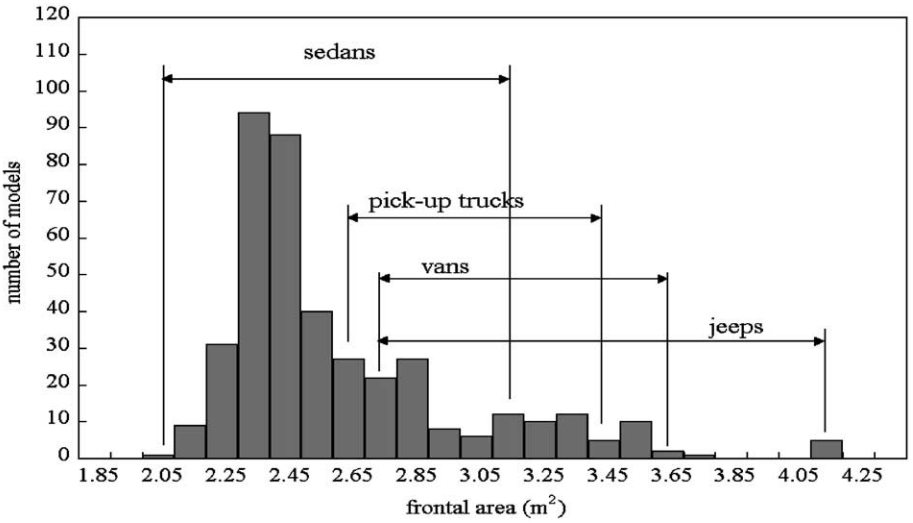

Fig. 6. The number of models of small-sized vehicles (length $\leqslant 7.6$ m) for sale in Taiwan in December 1996 versus vehicular frontal area. These data infer that the value of the averaged frontal area of small-sized vehicles is about $2.5\,m^2$.

studies [3,8,9] suggested that the averaged frontal area of modern small-sized vehicles (A_{vs}) lies between 2.31 and $2.8\,m^2$. A survey made in 1996 for the small-sized vehicles in Taiwan and the results (Fig. 6) show that sedans stand for the majority of the small-sized vehicles and the frontal areas of these vehicles fall in a range between 2.05 and $4.15\,m^2$. To estimate the averaged frontal area of these vehicles, we divide this range of area into 22 intervals of different frontal area. After weighted by the vehicle number, the averaged frontal area of the small-sized vehicles in Taiwan can be obtained to be $2.5\,m^2$, which is used as the averaged frontal area of small-sized vehicles in our study. The value of the averaged frontal area of large-sized vehicles is chosen as $7.11\,m^2$ in our study, which is about the frontal area of a bus. Besides the frontal area of vehicles, we also separate the drag coefficients of vehicles into two kinds, Cd_s and Cd_l, for small and large-sized vehicles, respectively. Although previous studies usually assigned them to be around 0.32 and 0.8, respectively [10–12], we know they actually should vary with traffic density. The values of all the parameters used in the present study are summarized in Table 1, except the four coefficients f, K_j, Cd_s, and Cd_l, which are determined by the optimization procedure.

3.2. Optimization procedure

With data that describe the traffic along the tunnel and parameters listed in Table 1, the governing equations (Eqs. (2)–(8)) can be solved for the time series of induced wind speed. However, the discussion in Section 3.1 has pointed out that there are four major coefficients; Cd_s, Cd_l, K_j, and f. These coefficients are of high-dependency on the real traffic condition and the design of the tunnel and therefore

Table 1
Values of parameters

ρ	1.16 kg/m^3 (30°C, 1 atm)
A_{vs}	2.5 m^2
A_{vl}	7.11 m^2
L	1762 m
A_t	93.88 m^2
D_h	10.38 m
K_{en}	0.6
θ_h	45°
A_F	2.01 m^2
V_F	30 m/s
N_F	3 (3:08–4:08, 8:08–9:08, 7/23/1997)
f	To be determined by the optimization procedure
Cd_s	
Cd_l	
K_j	

could not be measured or specified beforehand. To resolve this difficulty, we propose an optimization procedure to determine the most appropriate values of these four coefficients through careful examination of the agreement in magnitude, amplitude, and phase between the calculated and the measured time series of wind speed.

The specific optimization procedure is described below:

(1) Select one set of data that clearly records the dynamic traffic flow for a period of time (6 h for example), when the traffic was smooth and the traffic density maintained in a small limited range. The wind speed measured in the tunnel during the same period of time is also selected as the standard series to be checked with the computed result.
(2) Employ the group-partition dilemma [4] to transform the traffic-flow data measured at the outlet portal into the one standing for traffic in the tunnel.
(3) A rough estimation of the possible range of each of the four coefficients f, Cd_s, Cd_l, and K_j is made according to the knowledge of aerodynamics. One can skip K_j if no fan is turned on during the period of time analyzed. Assume the possible ranges of the four coefficients to be $f_{min} \leqslant f \leqslant f_{max}$, $Cd_{s\,min} \leqslant Cd_s \leqslant Cd_{s\,max}$, $Cd_{l\,min} \leqslant Cd_l \leqslant Cd_{l\,max}$, and $K_{j\,min} \leqslant K_j \leqslant K_{j\,max}$, the most appropriate value of each coefficient can be found from the discrete values given by the following equations:

$$f_i = f_{min} + (i-1)\,\Delta f, \quad i = 1, 2, 3, \ldots, n_f + 1, \tag{9}$$

$$Cd_{s,j} = Cd_{s\,min} + (j-1)\,\Delta Cd_s, \quad j = 1, 2, 3, \ldots, n_s + 1, \tag{10}$$

$$Cd_{l,k} = Cd_{l\,min} + (k-1)\,\Delta Cd_l, \quad k = 1, 2, 3, \ldots, n_l + 1, \tag{11}$$

$$K_{j,m} = K_{jmin} + (m-1)\,\Delta K_j, \quad m = 1, 2, 3, \ldots, n_k + 1, \tag{12}$$

where

$$\Delta f = \frac{f_{\max} - f_{\min}}{n_f}, \quad \Delta Cd_{\mathrm{s}} = \frac{Cd_{\mathrm{s}\max} - Cd_{\mathrm{s}\min}}{n_{\mathrm{s}}}, \quad \Delta Cd_{\mathrm{l}} = \frac{Cd_{\mathrm{l}\max} - Cd_{\mathrm{l}\min}}{n_{\mathrm{l}}}$$

and

$$\Delta K_j = \frac{K_{j\max} - K_{j\min}}{n_k}.$$

(4) Substitute the traffic-flow data obtained in step 2 along with a set of aerodynamic coefficients (f_i, $Cd_{\mathrm{s},j}$, $Cd_{\mathrm{l},k}$) into the mathematical model so that the corresponding time series of the tunnel wind speed can be calculated and this solution will be called "trial solution" hereafter. This trial solution is then compared with the measured time series of tunnel wind speed (the standard series) mentioned in step 1. Since both the trial solution and the measured standard series are of fluctuating kind, the agreement between them shall be checked on the phase, magnitude, and amplitude. The exact agreement on phase can be reached by careful synchronization of wind-speed and traffic-flow measurements. However, the exact agreement on the magnitude as well as the amplitude of both series would not be possible. Their best agreement can be properly indicated by the minimum value of the root-mean-square deviation $|\bar{\varepsilon}| \equiv \sqrt{\sum_{i=1}^{n_{\mathrm{v}}} \varepsilon_i^2 / n_{\mathrm{v}}}$, where ε_i is defined by Eq. (1) in which V_i^* and V_i account for the ith value of both the standard and the trial solution of wind speed, respectively, and n_{v} represents the number of data in time series while excludes those data in the time interval when fans are in operation. The calculation of the time series of the wind speed and the corresponding root-mean-square deviation is implemented for each set of aerodynamic coefficients (f_i, $Cd_{\mathrm{s},j}$, $Cd_{\mathrm{l},k}$), $i = 1, 2, 3, \ldots, n_f + 1$, $j = 1, 2, 3, \ldots, n_{\mathrm{s}} + 1$, $k = 1, 2, 3, \ldots, n_{\mathrm{l}} + 1$.

(5) Find the global minimum among all of the root-mean-square deviations calculated in step 4. The three coefficients corresponding to the minimum root-mean-square deviation are defined as the most appropriate coefficients that would make the best agreement between the calculated time series of wind speed and the standard measured one in both amplitude and magnitude. If the global minimum root-mean-square deviation cannot be found from the calculation, the estimated ranges of the three coefficients ($f_{\min} \leqslant f \leqslant f_{\max}$, $Cd_{\mathrm{s}\min} \leqslant Cd_{\mathrm{s}} \leqslant Cd_{\mathrm{s}\max}$, and $Cd_{\mathrm{l}\min} \leqslant Cd_{\mathrm{l}} \leqslant Cd_{\mathrm{l}\max}$) shall be redefined and the optimization procedure is then restarted from step 3 until the global minimum root-mean-square deviation is reached.

(6) Once the most appropriate values of the coefficients (f, Cd_{s}, Cd_{l}) are determined, the calculation of the time series of wind speed is implemented again by using these coefficients as well as different pressure-rise coefficients $K_{j,m}$ defined by Eq. (12). For each $K_{j,m}$, a time series of wind speed is calculated and the degree of its deviation from the standard measured one can be calculated by the mean deviation $\bar{\varepsilon} \equiv \sum_{i=1}^{n_{\mathrm{F}}} \varepsilon_i / n_{\mathrm{F}}$, where n_{F} is the number of wind-speed data in the time interval when the fans are in operation. Here, we employ the mean

value instead of the root-mean-square value to indicate the degree of deviation. This is because the addition of fan thrust shall primarily increase the magnitude, not the amplitude, of the wind speed. Therefore, the best agreement between the trial solution of wind speed and the standard measured one is defined at $\bar{\varepsilon} = 0$, and the most appropriate value of coefficient K_j can be determined accordingly.

To the authors' experiences, the global minimum root-mean-square deviation is usually not zero, implying that a perfect agreement between the trial solution of wind speed and the standard measured one is not actually available. This is understandable because the anemometer would inevitably be influenced by the vortices generated by passing vehicles and therefore would measure not purely the averaged wind speed in the tunnel. On the other hand, there are also some uncertainties in the traffic-flow data, such as the frontal area of each vehicle, the averaged speed of each vehicular group. The data, that describe the dynamic traffic flow in the tunnel, are calculated from the data measured at the outlet portal with some assumptions, and therefore would inevitably deviate more or less from the real one.

In order to eliminate the vortices-caused errors in the measured data of wind speed and the reckoned errors of the data that describe the traffic flow in the tunnel, and also to reveal the individual effect of each aerodynamic coefficient on the deviation value, a so-called "hide-and-seek" try is devised. In this try we would first generate a time series of tunnel wind speed by the mathematical ventilation model with a set of measured data that describe the dynamic traffic flow in the tunnel and with a set of clearly specified coefficients (f_0, $Cd_{s,0}$, $Cd_{l,0}$). If let this calculated time series of wind speed to substitute the measured one as the standard series in the optimization procedure, then it would be possible to find a trial solution of wind speed that has zero root-mean-square deviation to the standard series. In the meantime we can also clearly observe the individual effect of each of these coefficients on the time series of wind speed and on the root-mean square deviation.

To explain this "hide-and-seek" try, we adopt the traffic-flow data measured between 10:00:00 and 16:00:00 on 7/23/1997, shown in Fig. 3, and arbitrarily designate the coefficients f_0, $Cd_{s,0}$, and $Cd_{1,0}$ to be 0.020, 0.32, and 0.8, respectively. With these measured data of the dynamic traffic flow and these assigned values of the coefficients, the ventilation model of Fu-De Tunnel will predict that the time series of wind speed would be as shown by the bold line in Fig. 7. The calculated time series of wind speed is now provided as a standard series in which we have hidden a set of "most appropriate coefficients". Based on this standard series, the optimization procedure is then tried to seek those coefficients.

To show the influence of the aerodynamic coefficients on the solution of wind speed, we try to alternatively misplace the drag coefficients, Cd_s and Cd_l, to smaller values say 0.16 and 0.4, respectively. The predicted time series of wind speed would then be smaller than the standard one as shown by the two thinner lines. The results show that the vehicular drag coefficients would alter both the magnitude and the amplitude of the wind speed and that the deviations do exist between the standard series and the trial solutions, except when all the coefficients used are identical to those of the standard series.

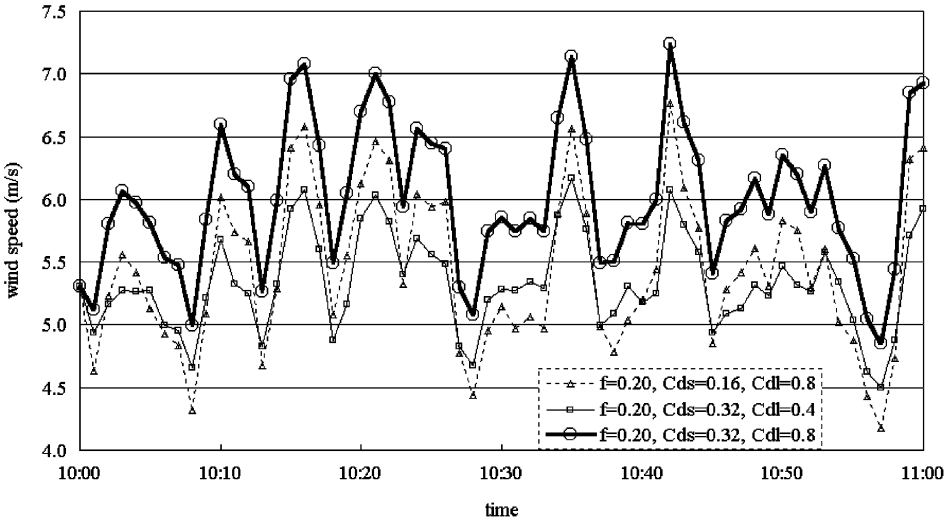

Fig. 7. The effect of the vehicular drag coefficients on the calculated wind speed. The traffic-flow data measured between 10:00 and 16:00 on 7/23/1997 are employed in the calculation. For a better resolution, only $\frac{1}{6}$ of the solution is shown.

According to the optimization procedure described above, we have now to select the ranges that the hidden values of coefficients f, Cd_s, and Cd_l will fall in. The ranges are obviously $0.011 \leqslant f \leqslant 0.031$, $0.176 \leqslant Cd_s \leqslant 0.496$, and $0.44 \leqslant Cd_l \leqslant 1.24$, which are uniformly divided into 21, 21, and 19 values, respectively. These discrete values of the three coefficients, f_i, $Cd_{s,j}$, and $Cd_{l,k}$, are then (0.011, 0.012, …, 0.020, …, 0.031), (0.176, 0.208, …, 0.32, …, 0.496), and (0.44, 0.48, …, 0.80, …, 1.24), respectively. For each discrete value of the friction coefficient f, there are 21×19 (or 399) pairs of discrete values of Cd_s and Cd_l that would be used to calculate the trial solutions of wind speed and the corresponding root-mean-square deviations. The minimum (a local minimum) among these deviation values and its corresponding pair of coefficients Cd_s and Cd_l are recorded in Fig. 8(a). For examples, as f_i is 0.011 the local minimum root-mean-square deviation would be 0.093 that occurs at $Cd_{s,j} = 0.208$ and $Cd_{l,k} = 0.600$, as f_i is 0.012 the local minimum root-mean-square deviation would be 0.088 that occurs at $Cd_{s,j} = 0.224$ and $Cd_{l,k} = 0.60$, and so on. Fig. 8(a) shows that as the friction coefficient increases from the lower limit (0.011) toward the hidden value (0.020), the local minimum root-mean-square deviation decreases from 0.093 toward 0.000 (the global minimum). At the global minimum, the drag coefficients Cd_s and Cd_l equal to their respective hidden values 0.32 and 0.8 and the trial solution is identical to the standard series. On the other hand, the further the friction coefficient goes beyond the hidden value (0.020), the larger is the local minimum root-mean-square deviation and the more is the deviation between the trial solutions and the standard series. In this case, we make a special arrangement to let the discrete values of f, Cd_s and Cd_l include their respective exact hidden values, i.e. 0.020, 0.32, and 0.8, respectively, so

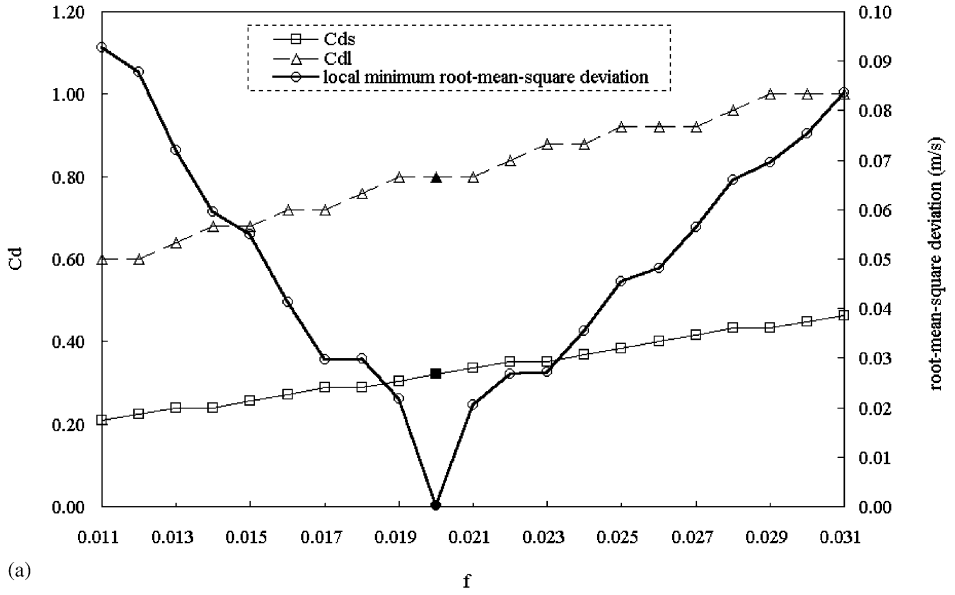

Fig. 8. The influence of discrete values of aerodynamic coefficients on the global minimum root-mean-square deviation. The time series of wind speed calculated by using the traffic-flow data measured in 10:00–16:00, 7/23/1997 and with $f = 0.020$, $Cd_s = 0.32$, and $Cd_l = 0.8$ is provided as a standard series. The other time series of wind speed calculated by using the same traffic-flow data but with other discrete values of aerodynamic coefficients are then compared with the standard series. The variation of the local minimums of root-mean-square deviation with the discrete values of the friction coefficient is shown in (a) and (b). (a) The discrete values of the three coefficients f, Cd_s, and Cd_l include the exact values of 0.020, 0.32, and 0.8, respectively, and a global minimum root-mean-square deviation of value zero can be obtained. (b) The discrete values of friction coefficient do not include the exact value, 0.020 and the global minimum root-mean-square deviation would not be zero and what can be obtained is just a set of most appropriate values of these coefficients from the location of the global minimum.

that a complete match of one of the trial solutions and the standard series can be seen.

However, for any given standard series without knowing its corresponding set of hidden values of these coefficients beforehand, the discrete values of each coefficient given by Eqs. (9)–(11) would inevitably more or less deviate from these hidden values. Under this situation, an exact agreement between trial solutions and the standard solution would not be possible and the global minimum of the root-mean-square deviation would not be zero, as shown in Fig. 8(b). Here, the discrete values of the coefficients Cd_s and Cd_l remain the same as before but those of coefficient f become 0.0115, 0.0125, …, 0.0195, 0.0205, …, 0.0315, which do not include the exact value of 0.020, the global minimum root-mean-square deviation is then 0.014 at $f = 0.0215$, $Cd_s = 0.336$, and $Cd_l = 0.84$. Although the values of these coefficients are not identical to their respective hidden values, they are close enough and would nevertheless be acceptable from the engineering point of view. For showing the variation of the root-mean-square deviation with respect to different discrete values of Cd_s and Cd_l, the calculation results around the global minimum are plotted in Figs. 9(a) and (b). Fig. 9(a) is suitable for vividly showing the variation of deviation value with respect to Cd_s and Cd_l, while Fig. 9(b) is suitable for locating the minimum deviation value and the corresponding drag coefficients and therefore figures of this kind would be used in the following studies.

4. Results and discussion

The optimization procedure is now employed to determine the most appropriate values of the aerodynamic coefficients of Fu-De Tunnel by using the data measured between 0:00 and 16:00 on 7/23/1997. These data are divided into three groups according to the different ranges of traffic densities: 0–3, 3–8, and 8–23 vehicles/lane/km, which were, respectively, measured in 0:00–6:00, 10:00–16:00, and 7:00–8:30. In the procedure, the time series of wind speed measured at 50 m from the outlet portal is selected as the standard series.

We now first apply the optimization procedure to analyze the data measured in 0:00–6:00 and to determine the most appropriate coefficients of the tunnel for the

Fig. 9. The distribution of the root-mean-square deviation around its global minimum in a case that a complete agreement between the two compared series is available. Here, the time series of wind speed calculated by using the traffic-flow data measured in 10:00–16:00, 7/23/1997 and with coefficients (f, Cd_s,Cd_l) = (0.020, 0.32, 0.8) (the hidden values) is served as a standard series. The other time series of wind speed calculated by using the same traffic-flow data and the same friction coefficient value but with different values of drag coefficients Cd_s and Cd_l are then individually compared with the standard series. The root-mean-square deviations are calculated and plotted in (a) as a surface plot, which shows clearly the variation of the root-mean-square deviation with respect to Cd_s and Cd_l. (b) The top view of the surface plot is shown for clearly showing the location of the minimum point. The minimum root-mean-square deviation is 0 m/s at $Cd_s = 0.32$ and $Cd_l = 0.8$. Each elliptical stripe in (a) and (b) represents a difference of deviation value of 0.05 m/s.

traffic density within the range 0–3 vehicles/lane/km. Since there were three jet fans tested between 3:08 and 4:08, at the early stage the optimization procedure is used to analyze the data of 0:00–3:08 and 4:08–6:00. According to the knowledge of tunnel ventilation and vehicle aerodynamics, we estimate that the most appropriate values

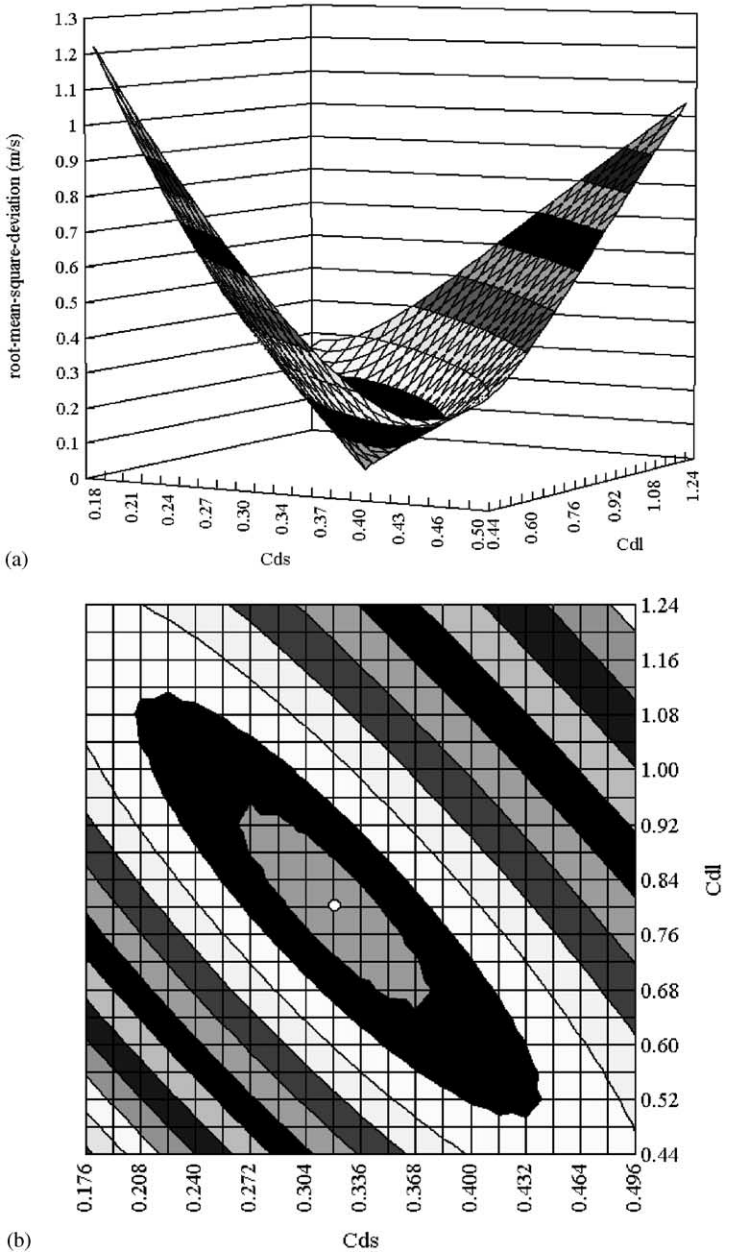

of the coefficients, f, Cd_s, and Cd_l, may fall within the ranges, $0.016 \leqslant f \leqslant 0.036$, $0.224 \leqslant Cd_s \leqslant 0.544$, and $0.08 \leqslant Cd_l \leqslant 0.88$. Please note that although it is strange to see a smaller value of Cd_l (0.08) than that of Cd_s (0.224), it would not have any influence on the most appropriate values of these coefficients. Each of these ranges is uniformly divided into 20 intervals (i.e. $n_f = n_s = n_l = 20$) in this study. The calculated results show that the global minimum root-mean-square deviation is 0.28m/s which occurs at $f = 0.026$, $Cd_s = 0.35$, $Cd_l = 0.36$, as shown by Figs. 10(a) and (b). Although these most appropriate values of coefficients f, Cd_s, and Cd_l are determined from the data measured in 0:00–3:08 and 4:08–6:00, they are also applicable to the period 3:08–4:08, because of the similar traffic density. With the most appropriate values of the three aerodynamic coefficients, the pressure-rise coefficient value of the jet fans is then determined by following step 6 of the optimization procedure. In this step, the calculation is performed for each of the discrete values of pressure-rise coefficient, K_j, which varies from 0.16 ($K_{j\,\min}$) to 1.06 ($K_{j\,\max}$) with an increment of 0.1. The mean deviation between the calculated and the standard measured time series of wind speed for each discrete value of K_j is plotted in Fig. 10(c), which clearly reveals that the most appropriate value of K_j is ≈ 0.56. In previous studies [3,8] the value of this coefficient falls within the range 0.8–1.0, which is evidently larger than what is found here for Fu-De Tunnel. This comparison reveals that the pressure-rise coefficient of jet fans may be highly circumstances dependent. The wind speed calculated by using these most appropriate values of coefficients f, Cd_s, Cd_l, and K_j is plotted in Fig. 10(d) which shows a very good agreement between the calculated and the measured wind speed. To be more specifically, the deviation between the two series of wind speed at every minute is indicated as a small circle in Fig. 10(d). These deviation data are further transformed into the discrete probability densities indicated by the outline circles in Fig. 5(a), which quite coincide with the density of a normal distribution function with a mean and standard deviations of -0.021 and 0.282 m/s, respectively. This reveals that the deviation between the calculated and the standard measured time series of wind speed is due to the uncertainties or errors which are harbored in the measured wind-speed and traffic-flow data and cannot be eliminated through the adjusting of the values of the coefficients.

The optimization procedure is next employed to analyze the data measured in another time period between 10:00 and 16:00, when the traffic density was within 3–8 vehicles/lane/km. We again estimate that the coefficients, f, Cd_s, and Cd_l may fall, respectively, within the ranges $0.016 \leqslant f \leqslant 0.036$, $0.224 \leqslant Cd_s \leqslant 0.554$, and $0.08 \leqslant Cd_l \leqslant 0.88$, and divide each of them uniformly into 20 intervals (i.e. $n_f = n_s = n_l = 20$), as for the previous case. The distribution of the root-mean-square deviation around the global minimum is plotted on $f - Cd_l$ and $Cd_s - Cd_l$ planes as shown by Figs. 11(a) and (b), respectively. The results show that the value of the global minimum root-mean-square deviation is 0.35 m/s that occurs at $f = 0.026$, $Cd_s = 0.32$, and $Cd_l = 0.4$. We surprisingly find that no matter at the present or the previous case the most appropriate value of the friction coefficient is found to be 0.026, which is pretty close to the value, 0.025, of other tunnels [3,8,9]. We also find that the increase of the traffic density from 0–3 to 3–8 vehicles/lane/km has

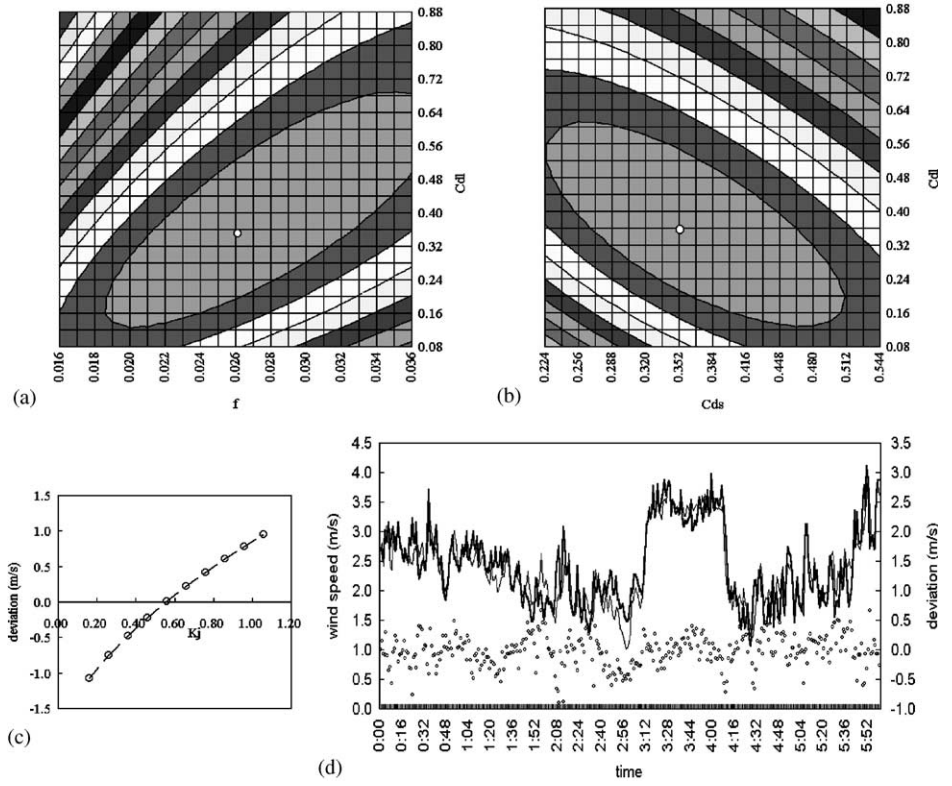

Fig. 10. Determination of the most appropriate values of the aerodynamic coefficients based on the data measured in 0:00–6:00, 7/23/1997, when the traffic density was within 0–3 vehicles/lane/km. The root-mean-square deviation around the global minimum is plotted on (a) the $f - Cd_l$ plane, and (b) the $Cd_s - Cd_l$ plane. In both (a) and (b), the global minimum root-mean-square deviation is 0.28 m/s and each elliptical stripe indicates a difference of 0.05 m/s. At the location of the global minimum, the coefficients f, Cd_s, and Cd_l have the most appropriate values which are 0.026, 0.35, and 0.36, respectively. (c) The effect of K_j on the mean deviation between the calculated and the standard measured series of wind speed is shown. The coefficient K_j has the most appropriate value of 0.56 at the zero mean deviation value. (d) Shows the comparison of the measured time series of wind speed (▬) and that calculated with a set of the most appropriate coefficient values (—). The small circles indicate the deviations between the two series.

reduced the averaged drag coefficient of small-sized vehicles from 0.35 to 0.32, which reflects a minor effect of tailgating [10]. The values 0.35 and 0.32 found here for the averaged drag coefficient of small-sized vehicles are consistent with that of a single modern sedan in references [11,12]. However, the averaged drag coefficient of large-sized vehicles is increased from 0.36 to 0.40, as the traffic density increases from 0–3 to 3–8 vehicles/lane/km, which seems to contradict the phenomenon of tailgating. If we want to make clear the reasons behind the contradiction, more intensive works to reduce the reckoned errors of the traffic-flow data are required. Since the traffic density and the percentage of the large-sized vehicles in the cases analyzed are low,

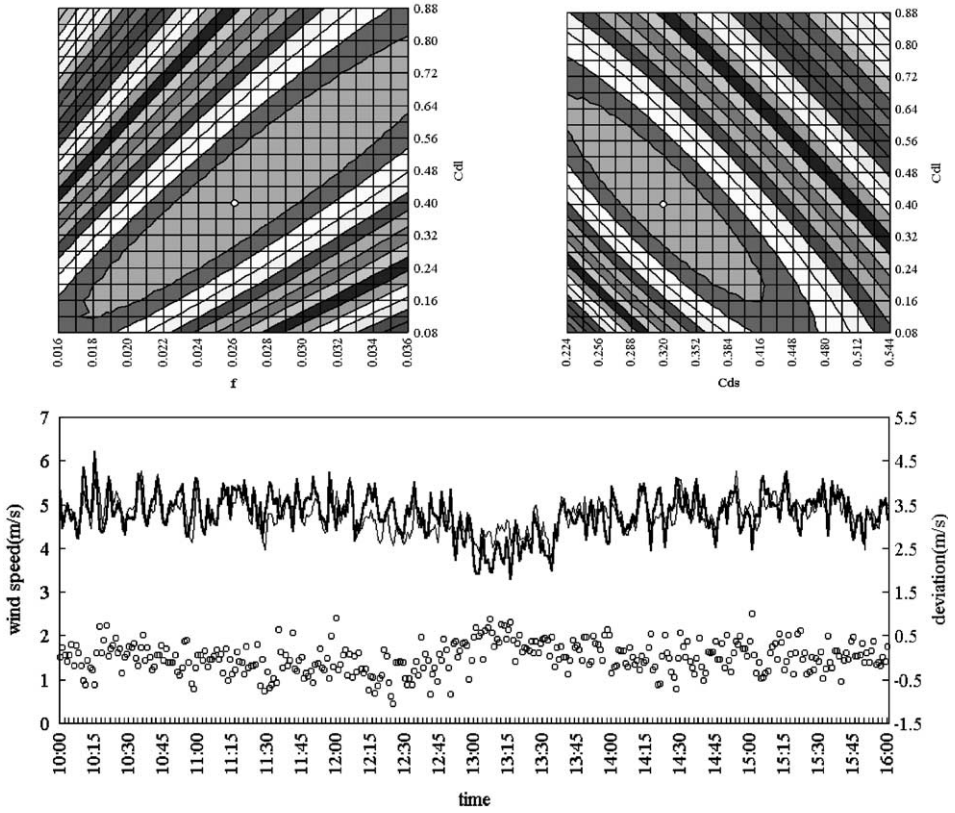

Fig. 11. Determination of the most appropriate values of the aerodynamic coefficients based on the data measured in 10:00–16:00, 7/23/1997, when the traffic density was within 3–8 vehicles/lane/km. The root-mean-square deviation around the global minimum is plotted on (a) the $f - Cd_l$ plane, and (b) the $Cd_s - Cd_l$ plane. In both (a) and (b), the global minimum root-mean-square deviation is 0.35 m/s and each elliptical stripe indicates a difference of 0.05 m/s. At the location of the global minimum, the coefficients f, Cd_s, and Cd_l have the most appropriate values which are 0.026, 0.32, and 0.40, respectively. (c) Shows the comparison of the measured time series of wind speed (▬▬) and that calculated with a set of the most appropriate coefficient values (—). The small circles indicate the deviations between the two series.

the effect of tailgating on large-sized vehicles is so little that may be overwhelmed by the traffic-flow reckoned errors. The averaged drag coefficient values found here for large-sized vehicles, 0.36 or 0.40, are only about half of the experimental value of a single tractor-trailer truck [12]. This result points out that generally the drag coefficient value of a large-sized vehicle would be obviously reduced after the vehicle enters the tunnel. We believe the reduction of this drag coefficient value is primarily due to suppression of the wake flow caused by the tunnel wall.

The time series of wind speed, which is calculated by using the most appropriate values 0.026, 0.32, and 0.4, respectively, for coefficients f, Cd_s, and Cd_l, is plotted in Fig. 11(c) to compare with the measured one. The results show that both of the two

time series of the wind speed are quite consistent with each other. The deviations between the two time series are also transformed into the discrete probability densities which are indicated by the outline circles in Fig. 5(b) and are almost coincide with that of a normal distribution function with a mean and standard deviations of -0.007 and 0.353 m/s, respectively.

The optimization analysis of the above cases with tunnel wind speed in 1.0–6.5 m/s ($6.02 \times 10^5 \leqslant Re \leqslant 3.9 \times 10^6$) has demonstrated that the value of the friction coefficient of Fu-De Tunnel is 0.026. According to the Moody diagram, this coefficient value and the corresponding range of the Reynolds number imply that the equivalent relative roughness of the tunnel is about 0.003 and the friction coefficient is a constant as long as the Reynolds number of the air flow is over 4×10^5. Since the wind speed measured between 7:00 and 8:30 is over 4 m/s ($Re \geqslant 2.4 \times 10^6$), it would be adequate to adopt the value 0.026 as the friction coefficient of the tunnel. On the other hand, the three jet fans, which were operated in 3:08–4:08, were started again simultaneously at 8:08, we therefore also adopt the value 0.56 as the pressure-rise coefficient of the three combined jet fans. The calculation is then focused on finding the most appropriate values for the drag coefficients of the large-sized as well as the small-sized vehicles from the data measured between 7:00 and 8:30. A few trials show that the most appropriate values of the averaged drag coefficients of small-sized and large-sized vehicles fall within the ranges $0.032 \leqslant Cd_s \leqslant 0.352$ and $0.08 \leqslant Cd_l \leqslant 0.88$, respectively. The calculated root-mean-square deviation is plotted in Fig. 12(a) which indicates that the minimum root-mean-square deviation, 0.293 m/s, occurs at $Cd_s = 0.20$, and $Cd_l = 0.24$. Both of the two values of drag coefficients are much smaller than those found from the data measured in the other two time periods. This result demonstrates that a strong tailgating effect does exist, as the traffic density is high enough. The time series of wind speed, which is calculated by using $f = 0.026$, $Cd_s = 0.20$, $Cd_l = 0.24$, and $K_j = 0.56$, is plotted in Fig. 12(b), which again shows that the computed result is in good agreement with the measured one. During the thrust developing period (8:08–8:17) of the three jet fans, the wind speed is increased from 4.1–5.6 m/s. The agreement between the calculated and the measured wind speed during this period reveals that the value 0.56 of the pressure-rise coefficient is appropriate. The discrete deviations between both time series of wind speed are again indicated by small circles, which in the present case have only 91 data. The discrete probability densities of these 91 deviation data are shown in Fig. 5(c) by outline circles, which again are pretty close to the density of a normal distribution function with mean $\mu = -0.041$ m/s and standard deviation $\sigma = 0.292$ m/s.

By comparing Figs. 10(a) and 11(a), we find that the root-mean-square deviation in Fig. 11(a) has a higher gradient with respect to the coefficients f and Cd_l. This is because that there are more amount of large-sized vehicles running in the tunnel during 10:00–16:00 than during 0:00–6:00, see Fig. 3(a). When the amount of large-sized vehicles increases, the influence of the drag coefficient Cd_l on the time series of computed wind speed and the corresponding root-mean-square deviation is augmented. Figs. 10(b), 11(b) and 12(a) also show that the more the amount of vehicles is in the tunnel, the steeper is the gradient of the root-mean-square deviation with respect to the drag coefficients. Each elliptical curve on these figures goes

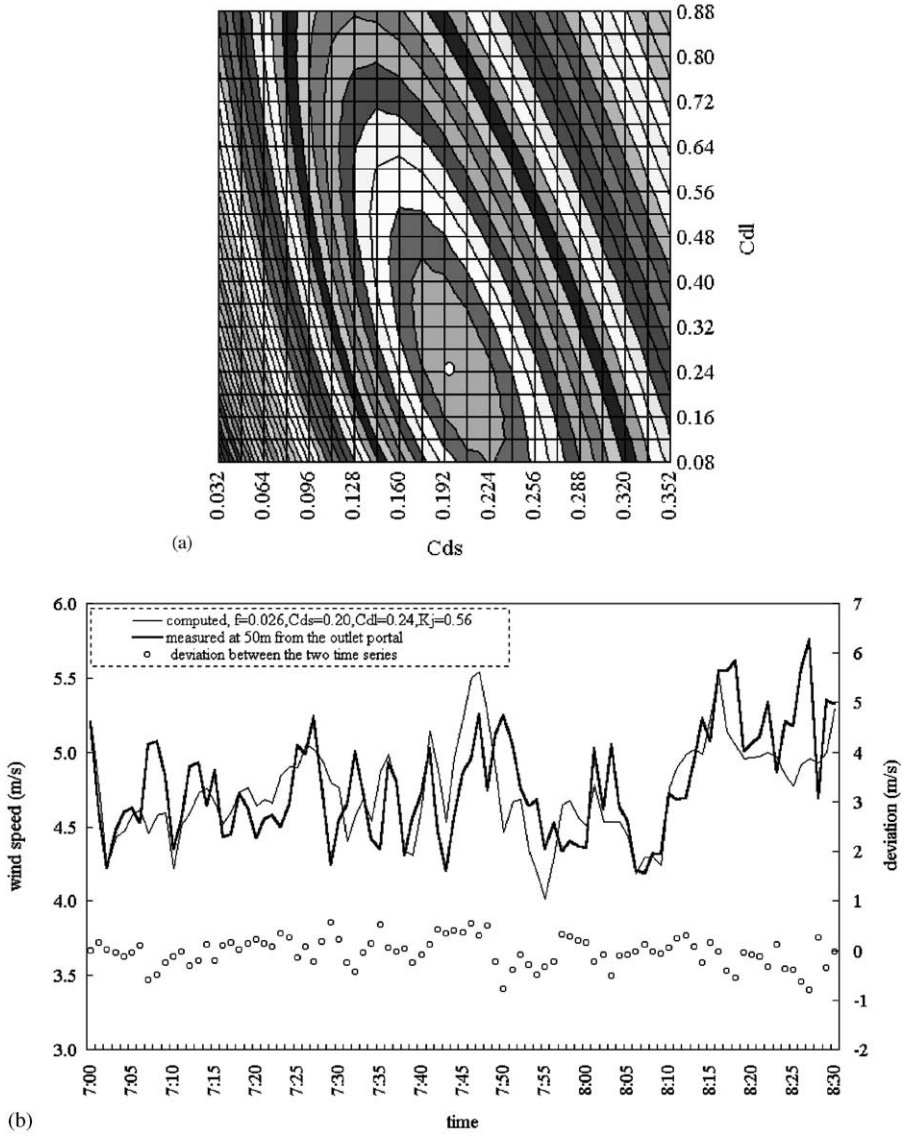

Fig. 12. Determination of the most appropriate values of the aerodynamic coefficients based on the data measured in 7:00–8:30, 7/23/1997, when the traffic density was within 8–23 vehicles/lane/km. (a) The root-mean-square deviation around the global minimum on the $Cd_s - Cd_l$ plane. In the calculation, the values of the friction coefficient and the pressure-rise coefficient of jet fans are given as 0.026 and 0.56, respectively. The minimum root-mean-square deviation is 0.293 m/s and each elliptical stripe on this figure indicates a difference of 0.05 m/s. The most appropriate values of coefficients Cd_s and Cd_l are 0.20 and 0.24, respectively. (b) Comparison of the measured time series of wind speed (▬) and that calculated with a set of the most appropriate coefficient values (—). The small circles indicate the deviations between the two series.

through all the points of the same root-mean-square deviation value. In each of the three figures, the elliptical curves have the same major axis, whose slope is intimately related to the relative amount of the small-sized and large-sized vehicles or the percentage of the small-sized vehicles in the tunnel.

5. Concluding remarks

The mean and standard deviations between the two time series of wind speed, which were simultaneously measured at two different locations in Fu-De Tunnel, fall approximately within the ranges 0.12–0.24 m/s and 0.16–0.23 m/s, respectively. The former is caused by the inherent errors of the anemometers and their associated instruments, and the latter is mostly caused by the vortices shed from the passing vehicles. The two deviation values are small. This result reveals that a good consistency does exist between the two time series of wind speed which were measured simultaneously at different locations and also reveal the high reliability of the measurement system and the incompressibility nature of the air flow in a highway tunnel.

The mean and standard deviations between the calculated and the measured series of wind speed are ≈ 0.0 and 0.28–0.35 m/s, respectively. This standard deviation is larger than that between the two measured series of wind speed. This is because it harbors not only the errors in the measured wind speed caused by the vortices shed from vehicles but also the errors in the calculated wind speed due to the minor uncertainties of the frontal area and the measured speed of each vehicle.

According to the optimization procedure, we find that the friction coefficient of Fu-De Tunnel is ≈ 0.026, when the wind speed is over 0.14 m/s or the Reynolds number is larger than 10^5. The averaged drag coefficients of the small-sized vehicles and the large-sized vehicles fall in the ranges 0.32–0.35 and 0.36–0.4, respectively, when the averaged traffic density in the tunnel is below 8 vehicles/lane/km and the vehicular tailgating effect is weak. However, as the averaged traffic density in the tunnel increases to 8–23 vehicles/lane/km during the morning rush hours, the averaged drag coefficients of the small-sized vehicles and the large-sized vehicles would be reduced to 0.20 and 0.24, respectively, revealing noticeable vehicular tailgating effects. Finally, the pressure-rise coefficient of jet fans, K_j, is found to be 0.56 which is almost traffic-density independent. Since the values of these coefficients are determined from the data measured at a full-scale tunnel operating under realistic highway traffic, they would possess most of the realistic features and are more practical than those measured by traditional ways.

Based on the data measured at Fu-De Tunnel, the optimization procedure has been shown to be effective on finding the most appropriate aerodynamic coefficients. We believe that the values of aerodynamic coefficients determined here for Fu-De Tunnel may also be applied to other tunnels of the same type under similar traffic conditions. Besides, the principle of the approach could also be further extended to determine the coefficients of tunnels of other types under other kind of traffic conditions.

Acknowledgements

This work has been supported by the Taiwan Area National Expressway Engineering Bureau, Ministry of Transportation and Communications through grant 860-NO73 and the National Science Council through grants NSC89-2212-E-034-002 and NSC89-2212-E-002-124.

Appendix A

The traffic density in a road tunnel is highly time dependent and so is its induced wind speed. The forces applied on the tunnel air by all the vehicles, tunnel wall, and auxiliary facilities in the tunnel would accelerate or decelerate not only the air in the tunnel but also that in the near surroundings. The third term on the right-hand side of Eq. (8) is to take this effect into account. This equation is derived from unsteady Bernoulli equation by assuming that the slope of the hill near the inlet portal of the tunnel is θ_h and the surrounding air there would flow into the tunnel in the same manner as a one-dimensional sink flow, see Fig. 13.

Since the cross-section area of the tunnel is A_t and the averaged wind speed in tunnel is V, the strength of the sink is therefore VA_t. According to the requirement of conservation of mass, the speed of the wind at a distance r from the center of the sink flow, V_r, can be written as

$$V_r = \frac{VA_t}{2(\pi - \theta_h)r^2}. \tag{A.1}$$

The unsteady Bernoulli equation can be written as [12,13]

$$P_\infty + \frac{\rho V_\infty^2}{2} + \rho g z_\infty = P_i + \frac{\rho V_i^2}{2} + \rho g z_i - \rho \int_{r_\infty}^{r_i} \frac{\partial V_r}{\partial t}\,\mathrm{d}r, \tag{A.2}$$

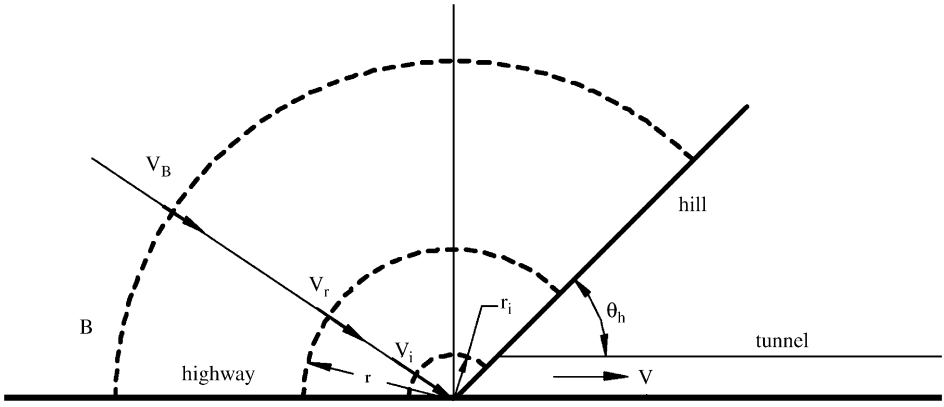

Fig. 13. The simplified one-dimensional sink flow around the inlet portal of a tunnel.

where V_∞ is the wind speed at a location far away from the inlet portal. At that location the atmospheric pressure and the elevation are P_∞ and z_∞, respectively. The wind speed V_∞ is usually negligible, and so is in the cases studied. As we select $z_\infty = 0$, P_∞ is then the atmospheric pressure on the elevation of the inlet portal. P_i and V_i are, respectively, the static pressure and wind speed on elevation z_i. The subscript "i" indicates that these quantities are at a distance r_i away from the center of the sink. The distance r_i is defined by the following equation so that the area of the partial spherical surface of radius r_i, shown by the inner dotted line in Fig. 13, would be identical to the cross-section area of the tunnel

$$r_i = \sqrt{\frac{A_t}{2(\pi - \theta_h)}}. \tag{A.3}$$

The wind speed V_i is therefore equal to the wind speed, V, in the tunnel. By making simplification according to the above discussion substituting Eq. (A.1) into Eq. (A.2) and, the following equation can be obtained:

$$\begin{aligned} P_i &= P_\infty - \frac{\rho V^2}{2} + \rho \frac{dV}{dt} \frac{A_t}{2(\pi - \theta_h)} \int_{r_\infty}^{r_i} \frac{1}{r^2}\, dr \\ &= P_\infty - \frac{\rho V^2}{2} - \rho \frac{dV}{dt} \frac{A_t}{2(\pi - \theta_h)} \left(\frac{1}{r_i} - \frac{1}{r_\infty} \right) \\ &\quad \text{where} \frac{1}{r_\infty} \approx 0 \\ &= P_\infty - \frac{\rho V^2}{2} - \rho \frac{dV}{dt} \sqrt{\frac{A_t}{2(\pi - \theta_h)}}. \end{aligned} \tag{A.4}$$

Here, the partial spherical surface of radius r_i serves as the inlet portal and the pressure P_i on that surface would be the same as P_{in} at the inlet portal. This blemish is inevitable as we try to catch some unsteady effects through the one-dimension simplification made for the flows inside and outside the inlet portal. Moreover, at the outlet portal of a tunnel, the abrupt change in the cross section of the flow implies that the value of the loss coefficient there is equal to 1.0 and the pressure there, P_{out}, is equal to the atmospheric pressure P_∞. Eq. (A.4) can be accordingly rewritten as

$$P_{in} = P_{out} - \frac{\rho V^2}{2} - \rho \frac{dV}{dt} \sqrt{\frac{A_t}{2(\pi - \theta_h)}}. \tag{A.5}$$

The third term on the right-hand side of the above equation is due to the inertial effect of the surrounding air, which may be minor for long tunnels but would play increasingly important role for shorter tunnels.

References

[1] F. Chen, H.M. Jang, Temperature rise in Ping-Lin Tunnel, J. Chin. Soc. Mech. Eng. 21 (4) (2000) 325–340.

[2] K.H. Huang, Transient analysis of the dispersion of vehicle pollution within a highway tunnel, Master Thesis, The University of Tennessee, Knoxville, December 1980.
[3] A. Mizuno, T. Sasamoto, I. Aoki, The emergency control of ventilation for the trans-Tokyo Bay Tunnel, Proceedings of the Seventh International Symposium on the Aerodynamics & Ventilation of Vehicle Tunnels, Brighton, UK, November 1991, pp. 365–384.
[4] H.M. Jang, F. Chen, A novel approach to the transient ventilation of road tunnels, J. Wind Eng. Ind. Aerodyn. 86 (2000) 15–36.
[5] F. Chen, H.M. Jang, Theoretical and experimental studies of ventilation in road tunnel, Technical Report #096-1, Taiwan Area National Expressway Engineering Bureau, Ministry of Transportation and Communications, December 1997.
[6] E. Kreyszig, Advanced Engineering Mathematics, 8th Edition, Wiley, New York, 1999.
[7] H.M. Jang, The effects of road tunnel ventilation coefficients—a graphical method, Proceedings of the 15th National Conference on Mechanical Engineering, The Chinese Society of Mechanical Engineers, Tainan, Taiwan, ROC, November 1998, pp.183–190.
[8] A. Mizuno, An optimal control with disturbance estimation for the emergency ventilation of a longitudinally ventilated road tunnel, Proceedings of the Third International Symposium on Fluid Control, Measurement and Visualization (FLUCOME '91), San Francisco, USA, 29–31 August 1991.
[9] Akisato Mizuno, Atsushi Ichikawa, Controllability of longitudinal air flow in transversely ventilated tunnels with multiple ventilation divisions, Proceedings of the First International Conference on Safety in Road and Rail Tunnels, Basel, Switzerland, 23–25 November 1992, pp. 425–437.
[10] A.J. Smits, A Physical Introduction to Fluid Mechanics, Wiley, New York, 2000.
[11] M.C. Potter, D.C. Wiggert, Mechanics of Fluids, Prentice-Hall, Englewood Cliffs, NJ, 1991.
[12] B.R. Munson, D.F. Young, T.H. Okiishi, Fundamentals of Fluid Mechanics, 2nd Edition, Wiley, New York, 1994.
[13] R.W. Fox, A.T. McDonald, Introduction to Fluid Mechanics, 5th Edition, Wiley, New York, 1998.